Available online www.jocpr.com

Journal of Chemical and Pharmaceutical Research, 2015, 7(12):452-469

Research Article

ISSN : 0975-7384
CODEN(USA) : JCPRC5

Comparison of different spatial interpolation methods for atmospheric pollutant PM2.5 by using GIS and Spearman correlation

Ping Zhang and Taotao Shen

School of Environmental and Chemical Engineering, Xi`an Polytechnic University, Xi`an, China

---

ABSTRACT

Accurate simulation of the spatial distribution of atmospheric pollutant PM2.5 is the basis of the air pollution control. This study uses PM2.5 concentration of 13 monitoring sites in Xi`an of China based on geographic information system (GIS) and Spearman correlation, application of inverse distance weighted (IDW), ordinary kriging (OK) and trend surface (TS) method, conducted the spatial interpolation analysis of PM2.5 concentration and comparison of the accuracy of different interpolation method. The results show that the accuracy of the IDW interpolation is the highest, the mean error (ME), the mean absolute error (MAE), the mean relative error (MRE), the root mean square error (RMSE) and the system error (SE) are 0.01, 0.05, 0.01, 0.31 and 0.01 respectively. The OK interpolation method is the lowest and the TS interpolation has higher accuracy. Correlation coefficient of simulated and observed value is 0.99 by IDW interpolation, while OK and TS interpolation are 0.62 and 0.67 respectively. The higher PM2.5 concentration areas distributed in the northern, southern and northeast while lower concentration zone located in the western and southeast.

Keywords: PM2.5, GIS, spatial interpolation, error analysis, Spearman correlation

---

INTRODUCTION

Atmospheric pollutant PM2.5 has the characteristics of easy to be toxic and harmful substances, resulting in human health damage and loss of the ecological environment, has become the focus of environmental pollution prevention and control in various countries [1-3].

However, the PM2.5concentration is difficult to obtain directly from remote sensing and monitoring site data can only represent the concentration of the site in a limited range, spatial distribution of PM2.5 need to use monitoring site data and interpolation analysis method based on GIS [4-6]. Spatial interpolation is an important method to estimate the unknown data by using the data of the known sample data. The commonly used spatial interpolation methods were inverse distance weighted (IDW), ordinary kriging (OK) and trend surface (TS) method [7-9]. Spatial interpolation distribution in the specific region, choose different interpolation methods to bring the different interpolation effect and accuracy [10-12]. However, there is little research on the error analysis of different spatial interpolation methods, and the research of Spearman and GIS in PM2.5 concentration interpolation is rarely reported, analyze the spatial interpolation of PM2.5 concentration by coupling of GIS and Spearman correlation is also rarely reported [13-15].

Therefore, this study application of geo-statistics in inverse distance weighted, ordinary kriging and trend surface method, spatial interpolation of atmospheric pollutant PM2.5 concentration based on GIS and Spearman correlation analysis, evaluation of the interpolation precision of different methods, comparing the correlation coefficient of monitoring and simulated values by different methods and proved optimal interpolation technology of atmospheric PM2.5 concentration in Xi'an of China. The results of the study have important theoretical and scientific significance for the spatial and temporal dynamic simulation of atmospheric pollutant PM2.5 concentration and air pollution control.

EXPERIMENTAL SECTION

2.1 The study area

The study area is located in Xi'an City, Shaanxi Province, China(E 107 ° 40 '- 109 ° 49, N 33 ° 42' - 34 ° 45 '), the area is 9983 square kilometers, which is a warm temperate semi humid continental monsoon climate, four seasons on temperature and humidity clearly. Annual average temperature and annual rainfall are 13.0-13.7 ℃, and 522.4-522.4 mm respectively, permanent population is 8.5529 million people (Figure 1).

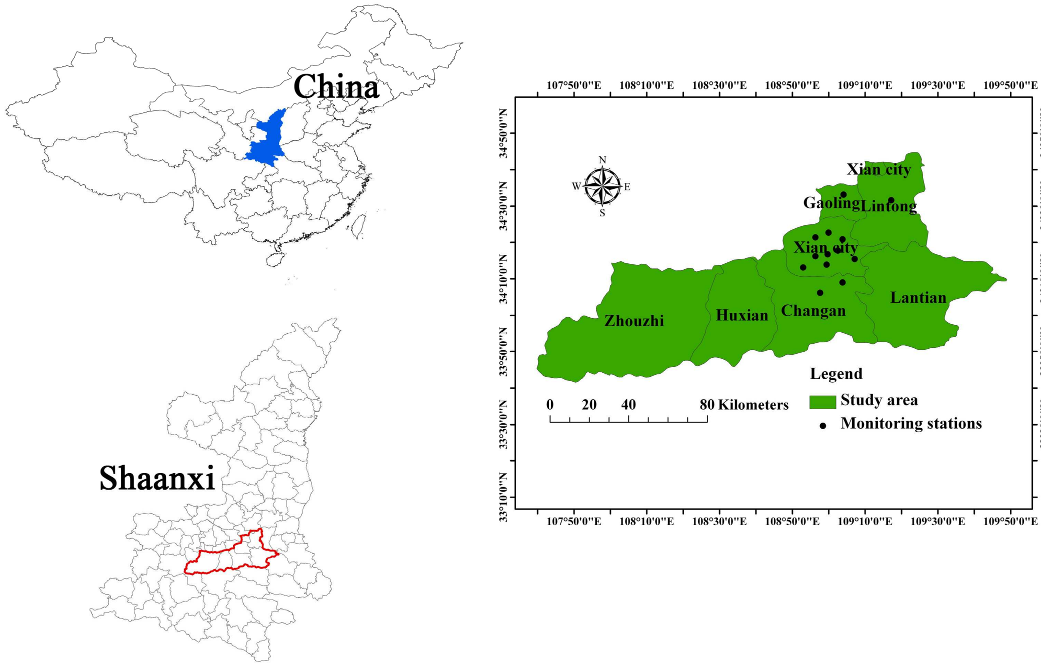

Figure 1. The study area

2.2 Spatial interpolation method based on GIS

2.2.1 Inverse distance weighted (IDW) interpolation method

The inverse distance weighted (IDW) interpolation is used to determine the pixel values by a linear combination of a set of sampling points, which is assumed to be reduced by the distance between the mapped variables and the sampling locations. The calculation formula is as follows:

$$Zo = [\sum_{i=1}^{n} \frac{Zi}{d_i^k}] \Big/ [\sum_{i=1}^{n} \frac{1}{d_i^k}] \tag{1}$$

Where, Z_o is the estimate value of o, Z_i is the value of the control point i, d_i is the distance between o and i, n is used in the estimation of the number of control points, k is the power of the specified.

2.2.2 Ordinary kriging (Kriging) method

Ordinary kriging method is assumed that sampling point between the distance or direction can reflect can be used to illustrate the spatial correlation of the surface changes, the mathematical function with the specified number of points or designated radius in all points were fitted to determine the location of each output value. The calculation formula is as follows:

$$Z_v^*(x) = \sum_{i=1}^{n} \lambda_i Z(x_i) \tag{2}$$

Where, $Z(x)$ is the measurement of the i position, and theλ_i is the unknown weight of the measurement value at the i position. x is the predicted position, and n is the number of measurements.

2.2.3 Trend surface (Trend) method

The trend surface analysis is a statistical method which is based on the known points in the space, and fitting a continuous mathematical surface, and studying the variation regularity of geological variables in the region and local area. The calculation formula is as follows:

$$Z = \beta_1 + \beta_2 x + \beta_3 y + \beta_4 x^2 + \beta_5 xy + \beta_6 y^2 + \cdots \tag{3}$$

Where, Z is the address variable, x and y are the coordinates of the observation points.

2.3 Error analysis of spatial interpolation

Error evaluation index mainly adopts mean error (ME), mean absolute error (MAE), mean relative error (MRE), root mean square error (RMSE) and the system error (SE). Among them, the mean error (ME) and mean absolute error (MAE) reflect the prediction error range, the mean relative error (MRE) reflect the accuracy of the predicted values for the measured values, the root mean square error (RMSE) reflect the sensitivity and extremum of the predicted value. The calculation formula is as follows:

2.3.1 Mean error (ME)

$$ME = \sum_{i=1}^{n}(\frac{y_i - x_i}{n}) \qquad (4)$$

2.3.2 Mean absolute error (MAE)

$$MAE = \sum_{i=1}^{n}\left|(\frac{y_i - x_i}{n})\right| \qquad (5)$$

2.3.3 Mean relative error (MRE)

$$MRE = \frac{1}{n}\left|\frac{\sum_{i=1}^{n}(y_i - x_{i)}}{y_i}\right| \qquad (6)$$

2.3.4 Root mean square error (RMSE)

$$RMSE = \sqrt{\frac{\sum_{i=1}^{n}(y_i - x_i)^2}{n}} \qquad (7)$$

2.3.5 System error (SE)

$$SE = \frac{\bar{y} - \bar{x}}{\bar{y}} \qquad (8)$$

Where, the average values of $\bar{y}$ and $\bar{x}$ for the measured and the predicted values.

2.4 The research data

In this paper, the collected data included daily value of PM2.5 concentration from 13 monitoring station in 2013, Xi'an of China. The monthly data were calculated by daily monitoring value of PM2.5 concentration.

RESULTS AND DISCUSSION

3.1 Spatial interpolation analysis of PM2.5 concentration based on inverse distance weighted (IDW) method of GIS

Spatial distribution of PM2.5 concentration in 13 monitoring station of Xi`an in 2013 by using the inverse distance weighted method of GIS as follows:

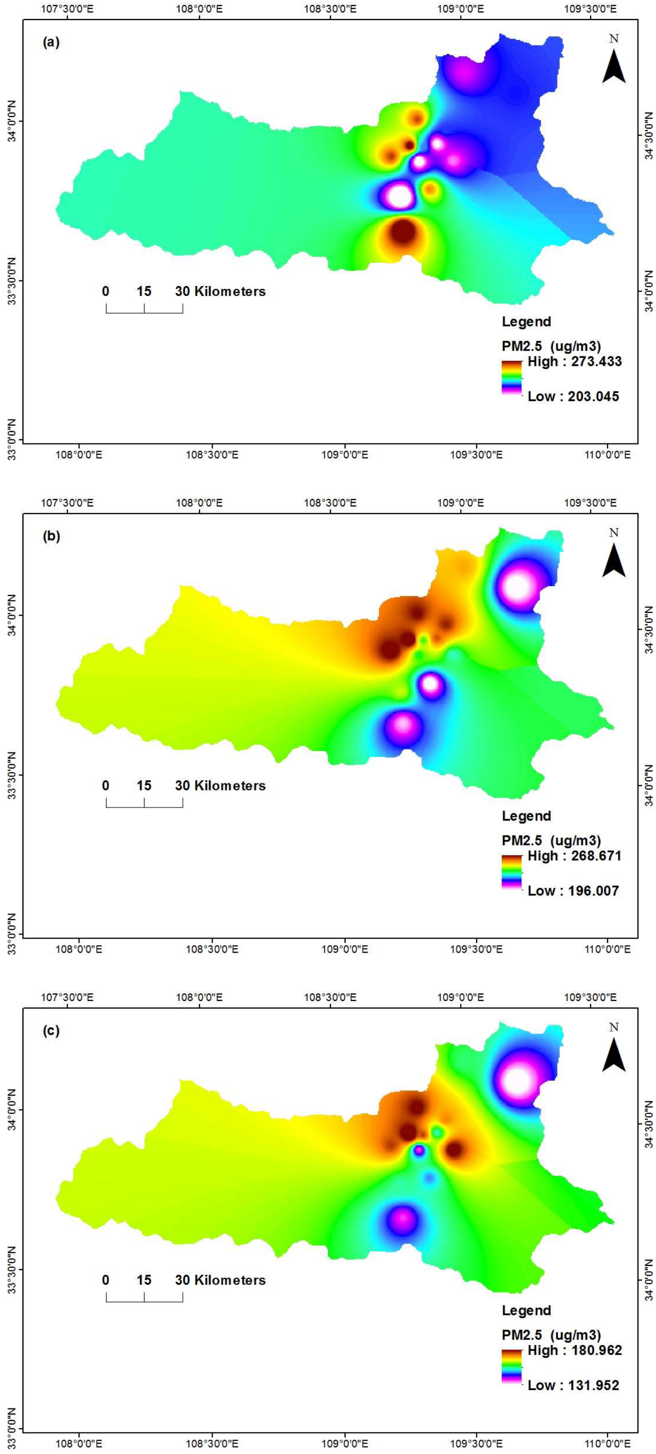
107°30'0"E
108°0'0"E
108°30'0"E
109°0'0"E
109°30'0"E
(a)
N
34°0'0"N
34°30'0"N
33°30'0"N
34°0'0"N
33°0'0"N
0 15 30 Kilometers
Legend
PM2.5 (ug/m3)
High : 273.433
Low : 203.045
108°0'0"E
108°30'0"E
109°0'0"E
109°30'0"E
110°0'0"E
(b)
Legend
PM2.5 (ug/m3)
High : 268.671
Low : 196.007
(c)
Legend
PM2.5 (ug/m3)
High : 180.962
Low : 131.952

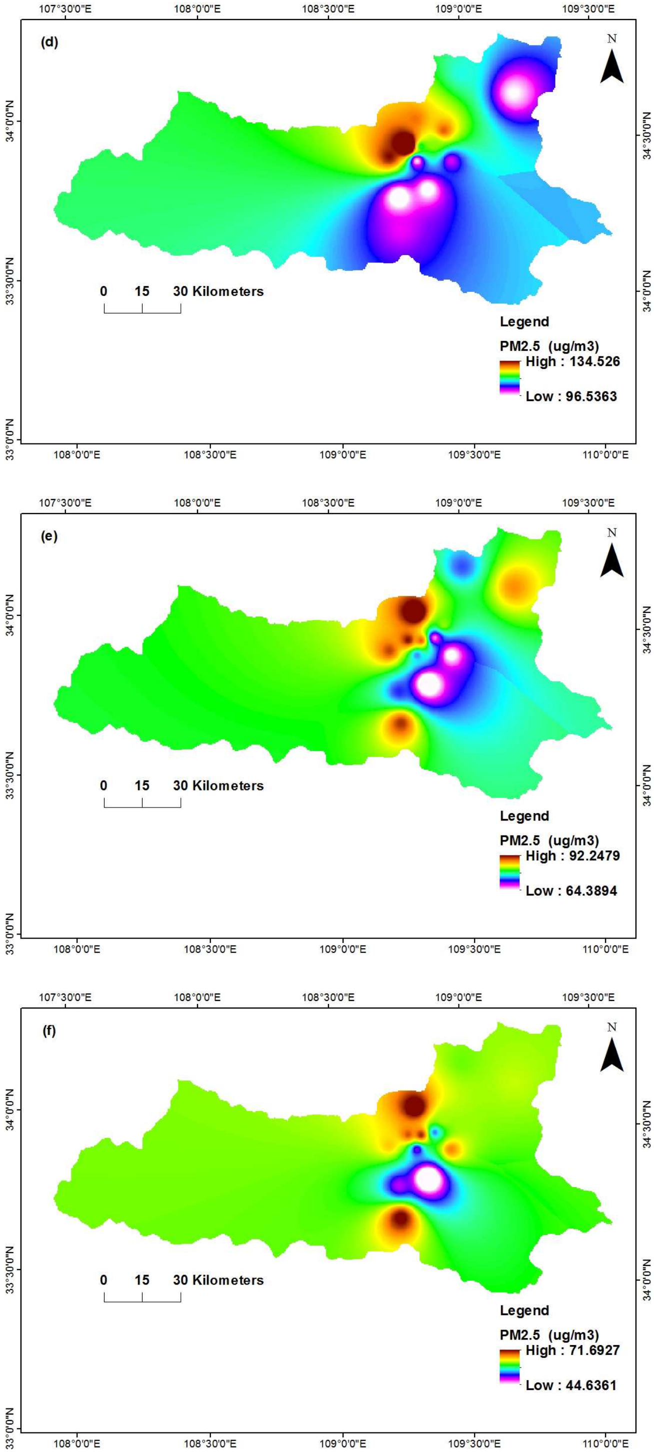
(d)
N
0 15 30 Kilometers
Legend
PM2.5 (ug/m3)
High : 134.526
Low : 96.5363
(e)
N
0 15 30 Kilometers
Legend
PM2.5 (ug/m3)
High : 92.2479
Low : 64.3894
(f)
N
0 15 30 Kilometers
Legend
PM2.5 (ug/m3)
High : 71.6927
Low : 44.6361
107°30'0"E
108°0'0"E
108°30'0"E
109°0'0"E
109°30'0"E
110°0'0"E
33°0'0"N
33°30'0"N
34°0'0"N
34°30'0"N

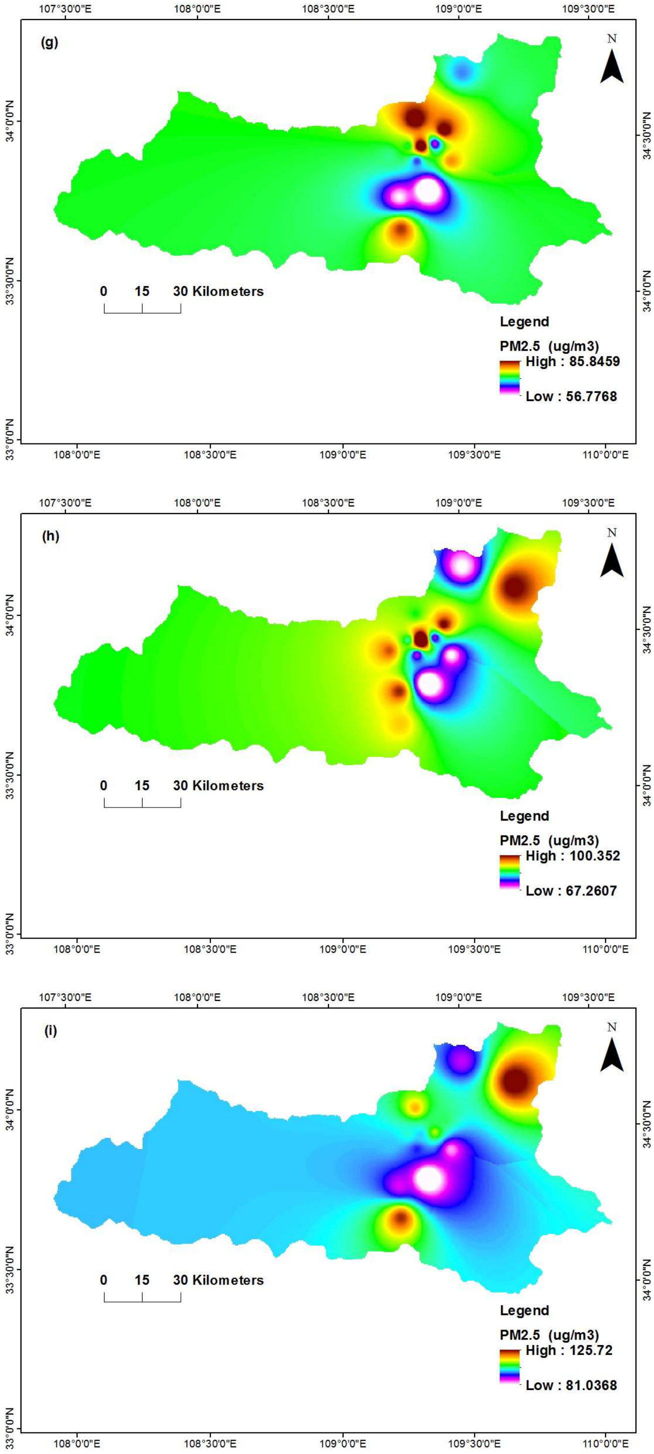
(g)
0 15 30 Kilometers
Legend
PM2.5 (ug/m3)
High : 85.8459
Low : 56.7768
(h)
0 15 30 Kilometers
Legend
PM2.5 (ug/m3)
High : 100.352
Low : 67.2607
(i)
0 15 30 Kilometers
Legend
PM2.5 (ug/m3)
High : 125.72
Low : 81.0368

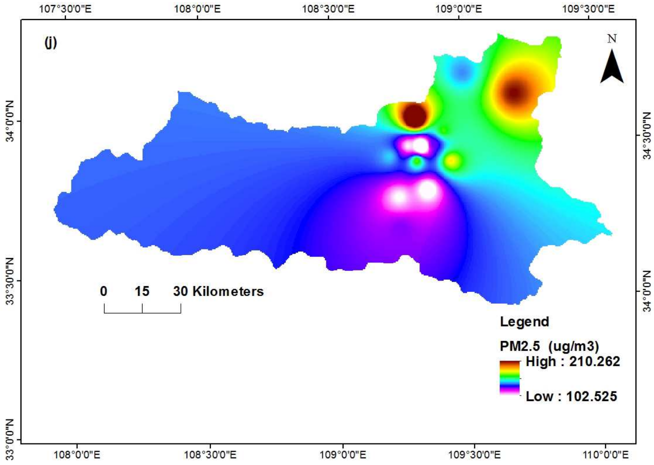
(j)
0 15 30 Kilometers
Legend
PM2.5 (ug/m3)
High : 210.262
Low : 102.525

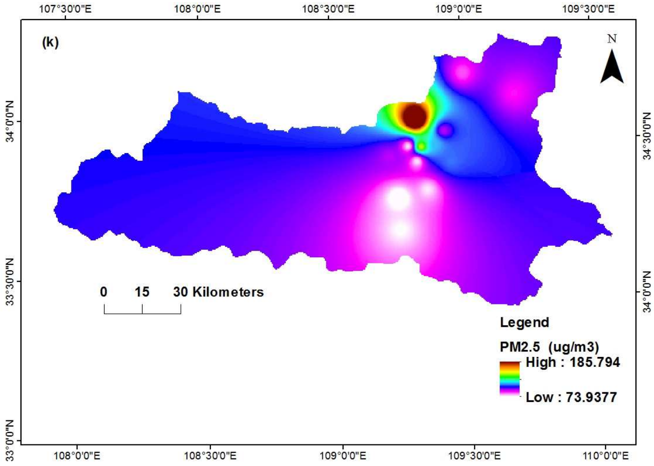
(k)
0 15 30 Kilometers
Legend
PM2.5 (ug/m3)
High : 185.794
Low : 73.9377

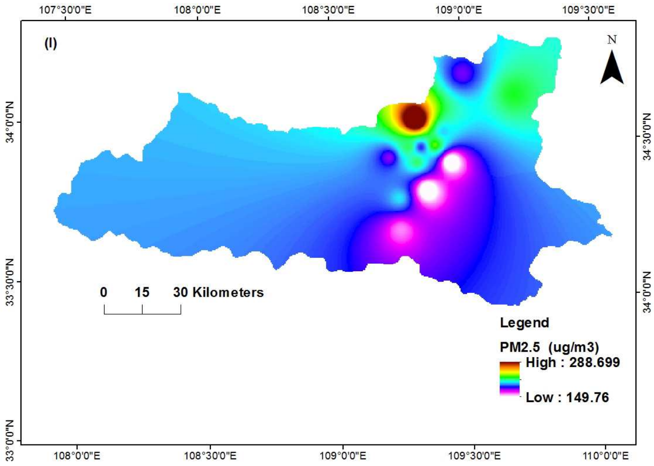
(l)
0 15 30 Kilometers
Legend
PM2.5 (ug/m3)
High : 288.699
Low : 149.76

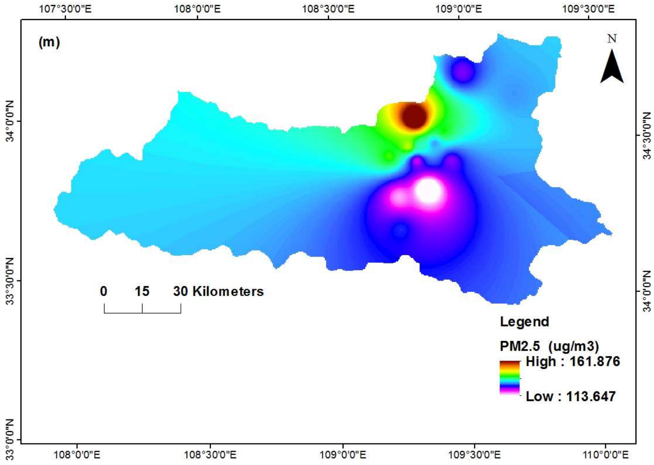

Figure 2. Spatial distribution of PM2.5 concentration based on IDW of GIS

(a: January, b: February, c: March, d: April, e: May, f: June, g: July, h: August, i : September, j: October, k: November, l: December m: monthly average. Unit: μg/m^3)

The Figure 2 shows that the range of PM2.5 concentration is 203.045-273.433 μg/m^3 in January, higher concentration mainly located in the central areas, moderate concentration mainly distributed in the southwest zone and lower concentration mainly located in the northeast areas. In October, the range of PM2.5 concentration is 102.506-102.506 μg/m^3, higher concentration mainly distributed in the northeast areas, the moderate concentration mainly located in the west and southeast zone and lower concentration distributed in central areas. Monthly average of PM2.5 concentration is range from 113.384 to 161.497 μg/m^3, higher concentration mainly located in the north-central areas, moderate concentration mainly distributed in the eastern and western zone and low concentration mainly located in the central-south areas. In general, the visual effect of PM2.5 concentration spatial distribution by inverse distance weighted interpolation is well.

3.2 Spatial interpolation analysis of PM2.5 concentration based on ordinary kriging (Kriging) method of GIS

Spatial distribution of PM2.5 concentration in 13 monitoring station of Xi`an in 2013 by using the ordinary kriging method of GIS as follows:

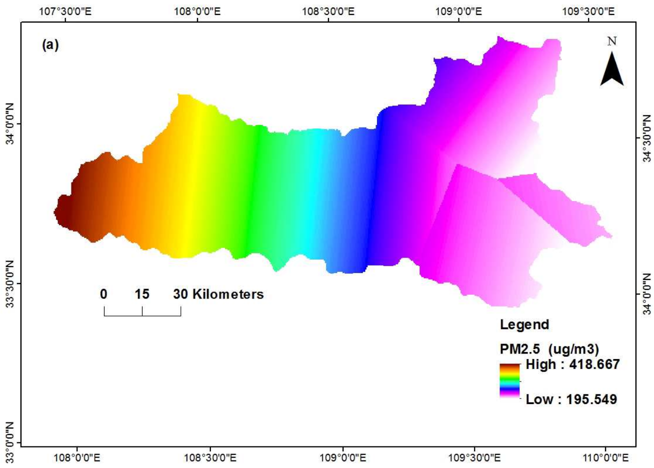

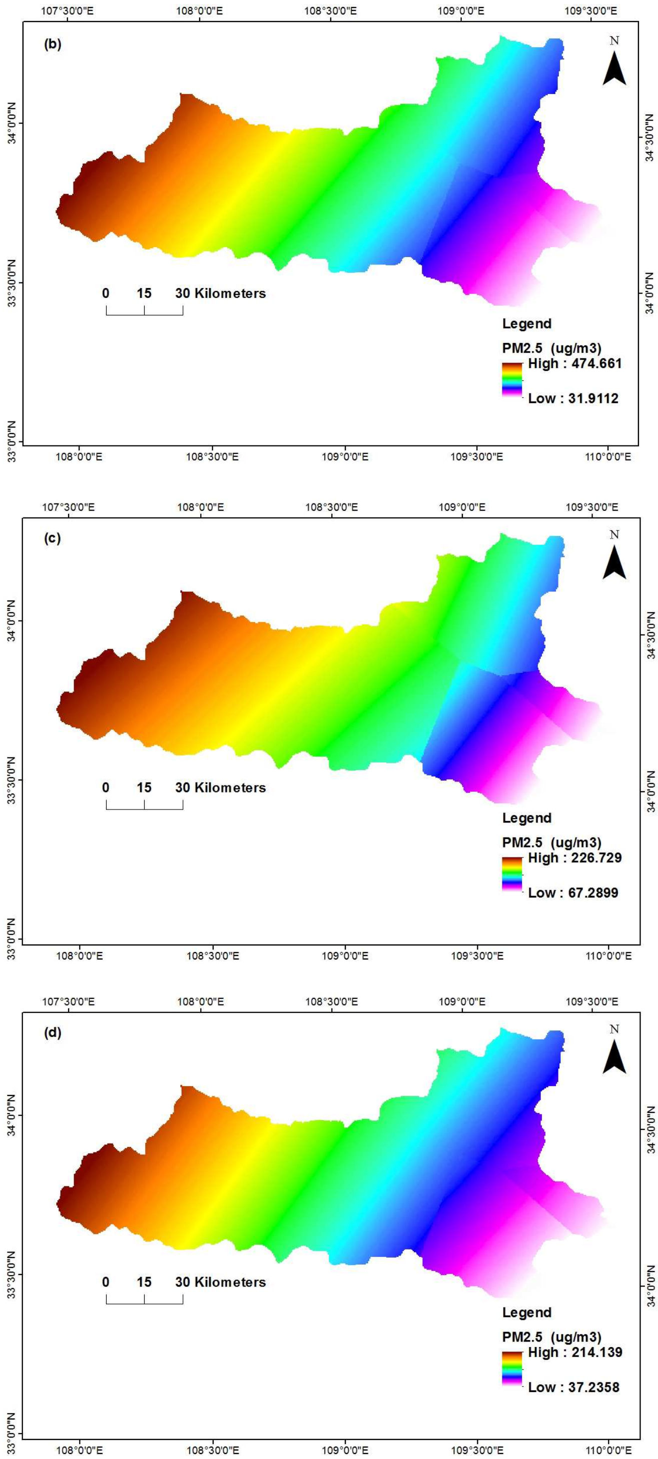
(b)
N
0 15 30 Kilometers
Legend
PM2.5 (ug/m3)
High : 474.661
Low : 31.9112
(c)
N
0 15 30 Kilometers
Legend
PM2.5 (ug/m3)
High : 226.729
Low : 67.2899
(d)
N
0 15 30 Kilometers
Legend
PM2.5 (ug/m3)
High : 214.139
Low : 37.2358

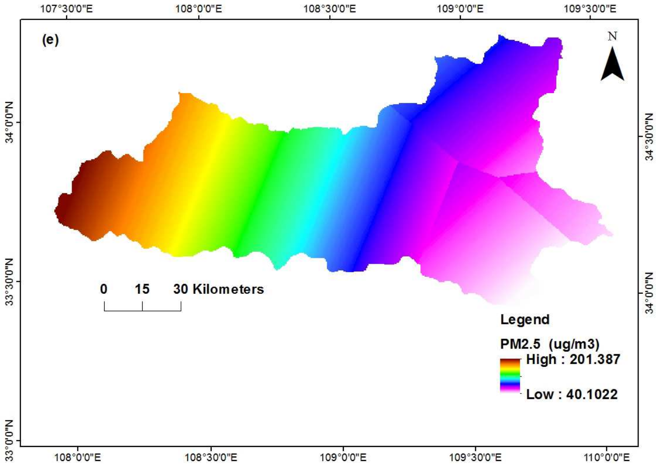
(e)
107°30'0"E
108°0'0"E
108°30'0"E
109°0'0"E
109°30'0"E
34°0'0"N
33°30'0"N
33°0'0"N
34°30'0"N
34°0'0"N
0 15 30 Kilometers
Legend
PM2.5 (ug/m3)
High : 201.387
Low : 40.1022
108°0'0"E
108°30'0"E
109°0'0"E
109°30'0"E
110°0'0"E

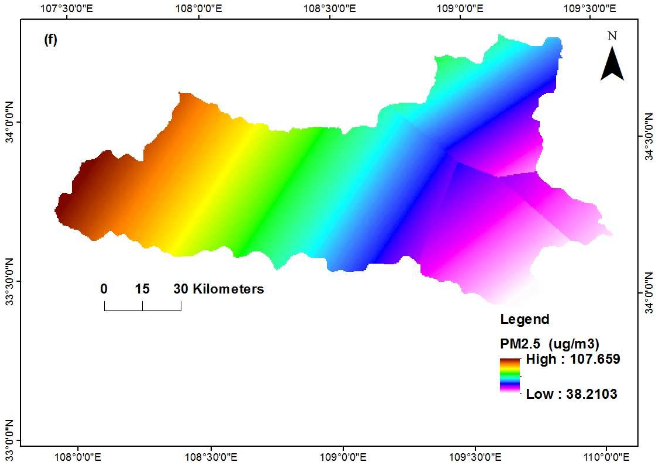
(f)
107°30'0"E
108°0'0"E
108°30'0"E
109°0'0"E
109°30'0"E
34°0'0"N
33°30'0"N
33°0'0"N
34°30'0"N
34°0'0"N
0 15 30 Kilometers
Legend
PM2.5 (ug/m3)
High : 107.659
Low : 38.2103
108°0'0"E
108°30'0"E
109°0'0"E
109°30'0"E
110°0'0"E

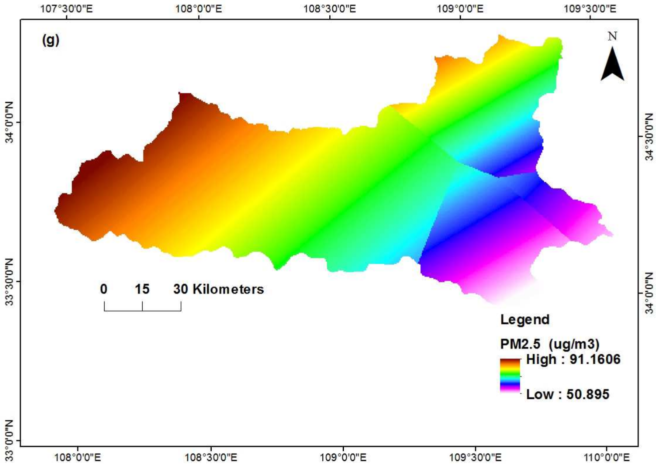
(g)
107°30'0"E
108°0'0"E
108°30'0"E
109°0'0"E
109°30'0"E
34°0'0"N
33°30'0"N
33°0'0"N
34°30'0"N
34°0'0"N
0 15 30 Kilometers
Legend
PM2.5 (ug/m3)
High : 91.1606
Low : 50.895
108°0'0"E
108°30'0"E
109°0'0"E
109°30'0"E
110°0'0"E

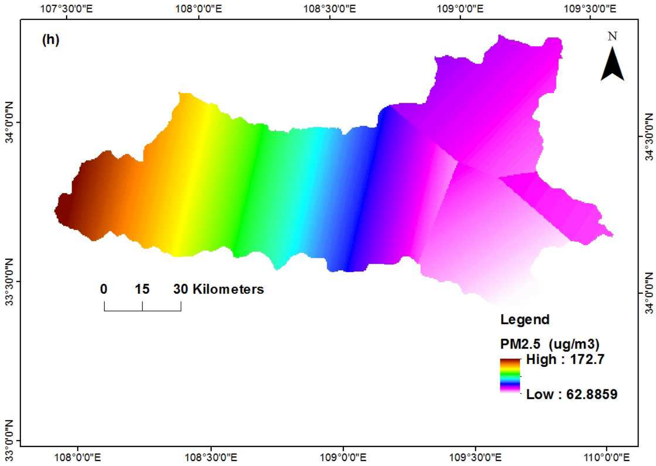
(h)
0 15 30 Kilometers
Legend
PM2.5 (ug/m3)
High : 172.7
Low : 62.8859

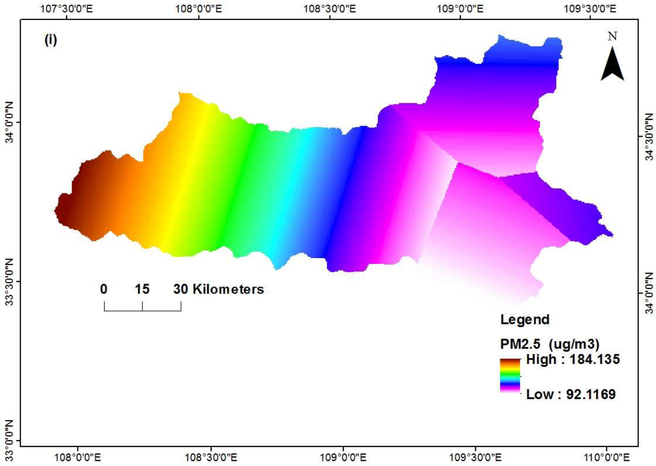
(i)
0 15 30 Kilometers
Legend
PM2.5 (ug/m3)
High : 184.135
Low : 92.1169

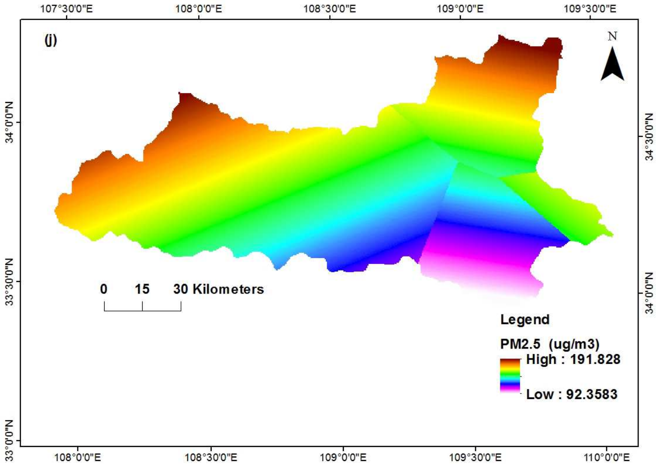
(j)
0 15 30 Kilometers
Legend
PM2.5 (ug/m3)
High : 191.828
Low : 92.3583

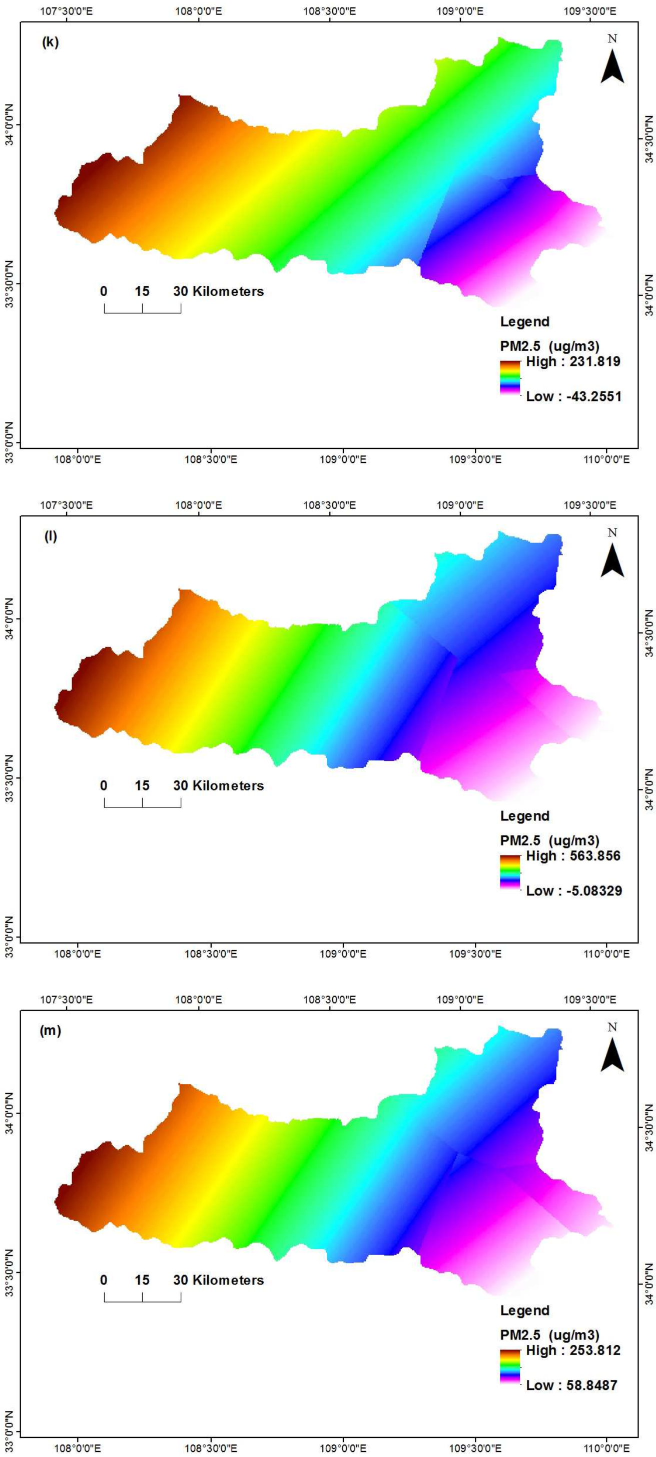

Figure 3. Spatial distribution of PM2.5 concentration based on Kriging of GIS

(a: January, b: February, c: March, d: April, e: May, f: June, g: July, h: August, i : September, j: October, k: November, l: December m: monthly average. Unit: $\mu g/m^3$)

The Figure 3 shows that the range of PM2.5 concentration in February is 31.9112-474.661 $\mu g/m^3$, higher concentration mainly distributed in the western areas, the moderate concentration mainly located in the central zone and lower concentration mainly distributed in the south-east. In November PM2.5 is range from 43.2551 to 231.819 $\mu g/m^3$, higher concentration mainly located in the western areas, moderate concentration mainly distributed in the central and northeast areas and lower concentration mainly located in the south-east. Monthly average of PM2.5 concentration is range from 58.8487 to 253.812 $\mu g/m^3$, higher concentration mainly distributed in the western zone, moderate concentration mainly located in the central and northeast areas and lower concentration mainly distributed in the south-east. Relatively speaking, visual effect of the spatial distribution of PM2.5 concentration by ordinary kriging method is general.

3.3 Spatial interpolation analysis of PM2.5 concentration based on trend surface (Trend) method of GIS
Spatial distribution of PM2.5 concentration in 13 monitoring station of Xi`an in 2013 by using the trend surface method of GIS as follows:

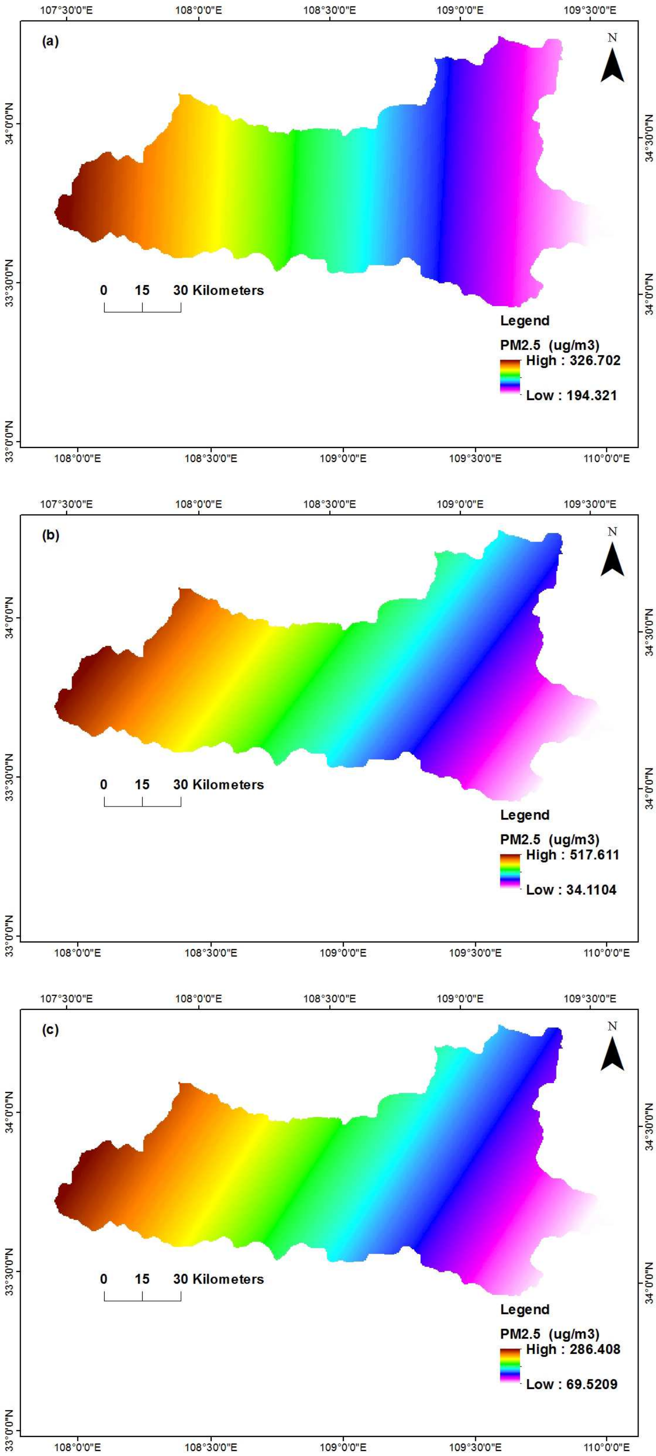

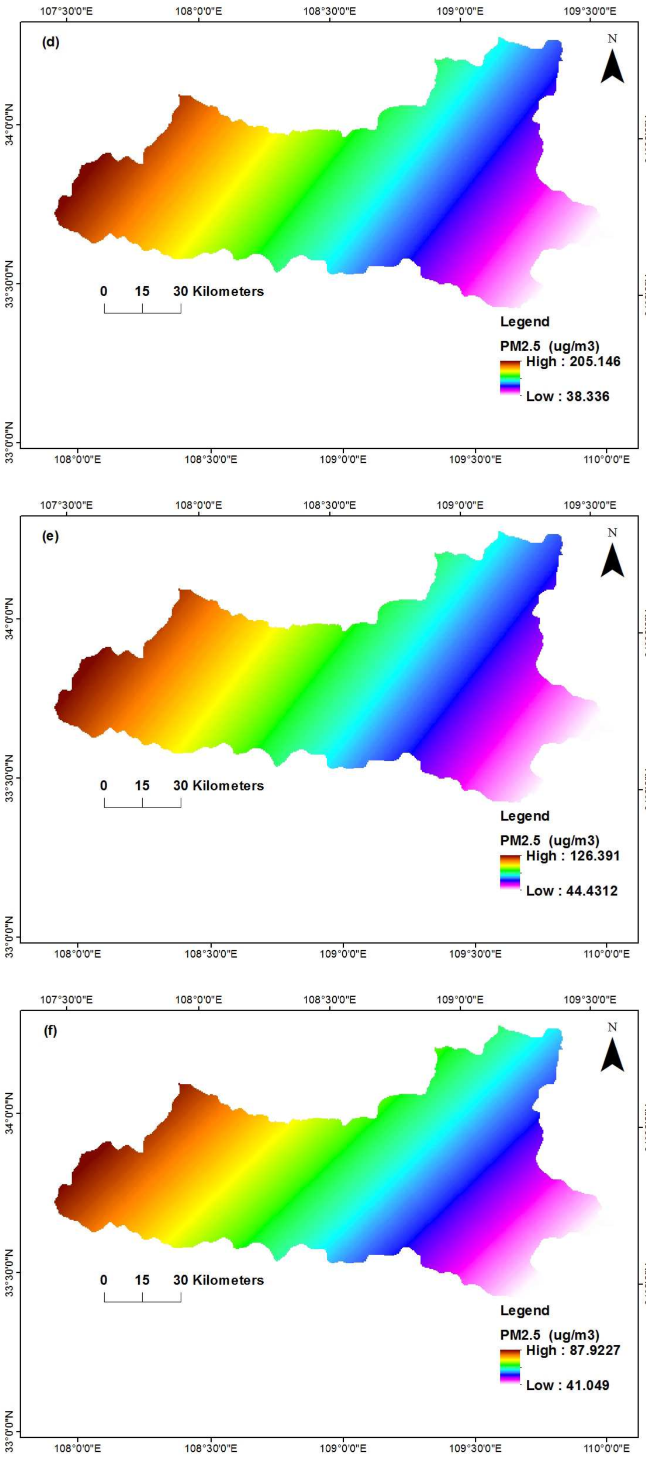
(d)
0 15 30 Kilometers
Legend
PM2.5 (ug/m3)
High : 205.146
Low : 38.336
(e)
0 15 30 Kilometers
Legend
PM2.5 (ug/m3)
High : 126.391
Low : 44.4312
(f)
0 15 30 Kilometers
Legend
PM2.5 (ug/m3)
High : 87.9227
Low : 41.049

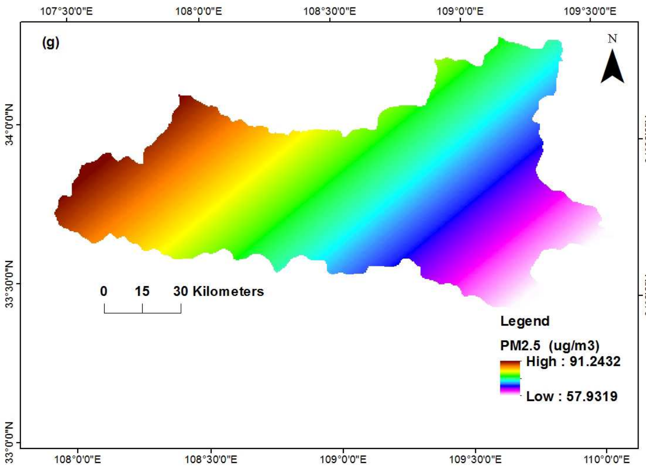
(g)
0 15 30 Kilometers
Legend
PM2.5 (ug/m3)
High : 91.2432
Low : 57.9319

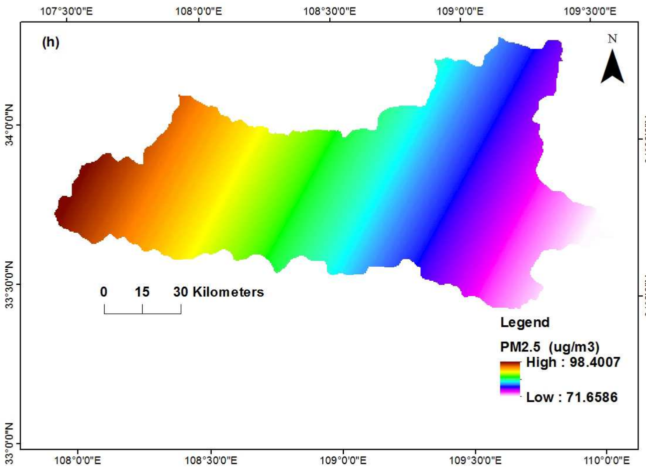
(h)
0 15 30 Kilometers
Legend
PM2.5 (ug/m3)
High : 98.4007
Low : 71.6586

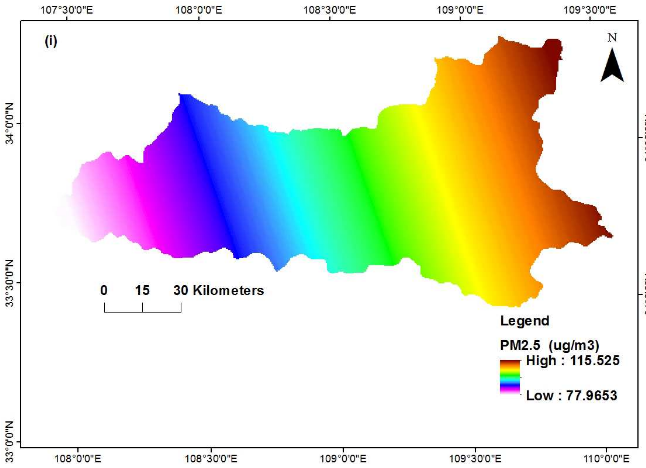
(i)
0 15 30 Kilometers
Legend
PM2.5 (ug/m3)
High : 115.525
Low : 77.9653

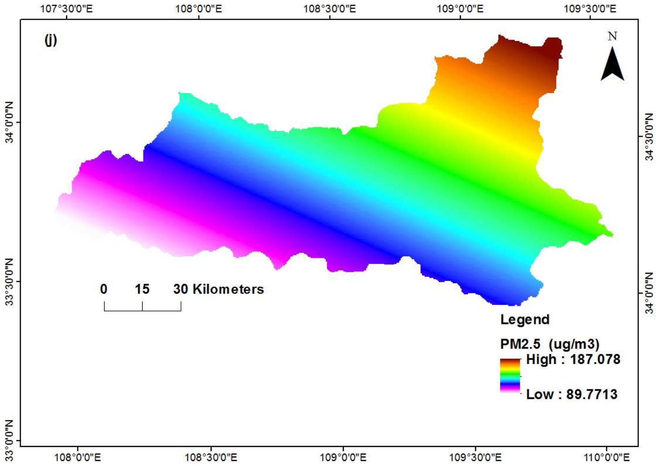
(j)
0 15 30 Kilometers
Legend
PM2.5 (ug/m3)
High : 187.078
Low : 89.7713

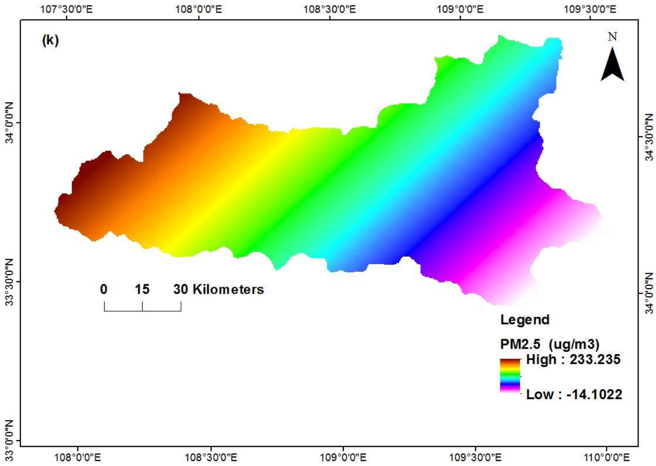
(k)
0 15 30 Kilometers
Legend
PM2.5 (ug/m3)
High : 233.235
Low : -14.1022

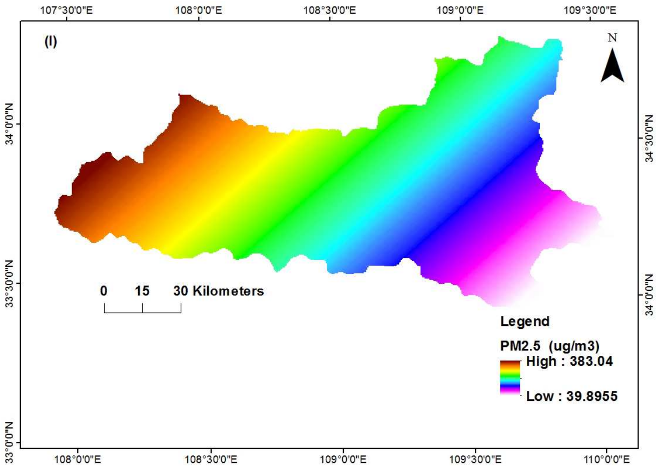
(l)
0 15 30 Kilometers
Legend
PM2.5 (ug/m3)
High : 383.04
Low : 39.8955

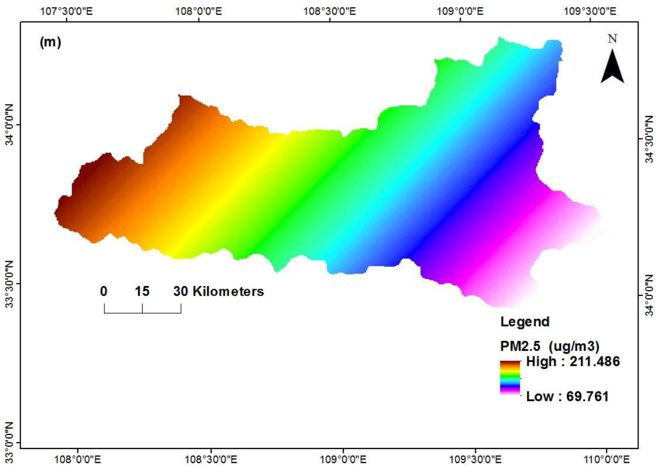

Figure 4. Spatial distribution of PM2.5 concentration based on Trend of GIS

(a: January, b: February, c: March, d: April, e: May, f: June, g: July, h: August, i : September, j: October, k: November, l: December m: monthly average. Unit: μg/m³)

The Figure 4 shows that the range of PM2.5 concentration in March is 69.5209-286.408 μg/m^3, higher concentration mainly distributed in the western zone, moderate concentration mainly located in the central and northeast areas and lower concentration mainly distributed in the south-east. The range of PM2.5 concentration in December is 39.8955-39.8955 μg/m^3, higher concentration mainly located in the western areas, moderate concentration mainly distributed in the central and northeast areas and lower concentration mainly located in the south-east zone. Monthly average of PM2.5 concentration is range from 69.761 to 211.486 μg/m^3, higher concentration mainly located in the western areas, moderate concentration mainly distributed in the central and northeast zone, lower concentration mainly located in the south-east. In general, the visual effect of spatial distribution of PM2.5 concentration by trend surface interpolation is better.

3.4 The error analysis of different interpolation method

The mean error (ME), mean absolute error (MAE), mean relative error (MRE), mean square error (RMSE) and systematic error (SE) of different interpolation methods are shown in Table 1. RMSE of inverse distance weighted (IDW) method is 0.31, comparatively speaking, ordinary kriging (Kriging) and trend surface (Trend) method were 8.79 and 8.44 respectively, indicating that the inverse distance weighted method is more sensitive than the other two methods. On the whole, the inverse distance weighted method is better than the other two methods whether it is from the error range of the forecast value, the accuracy of the predicting value relative to the observed value, or the sensitivity and the reflection of the simulated value.

Table 1 The error parameter values of three interpolation methods

Error evaluation index	IDW	Kriging	Trend
ME	0.01	0.55	0.05
MAE	0.05	6.89	6.45
RMSE	0.31	8.79	8.44
SE	0.01	0.42	0.04
MRE	0.01	0.34	0.04

3.5 Correlation analysis of different interpolation methods

The correlation coefficient was used to evaluate the correlation between the simulated and the observed data of PM2.5 concentration based on the Spearman correlation analysis of SPSS, and the results are shown in Table 2. The results in Table 2 show that the correlation coefficient of simulated and observed value of is the largest by IDW is 0.99, in contrast, correlation coefficient of predicted and measured value is minimum is 0.62 by ordinary kriging, and the correlation coefficient of simulated and observed value is 0.67 by trend surface, indicating that correlation coefficient of trend surface and the ordinary kriging method has less precision than the inverse distance weighted method.

Table 2 Correlation coefficient of PM2.5 concentration by different interpolation methods based on the Spearman correlation analysis

	IDW	Kriging	Trend
IDW	1.00	0.62	0.67
Kriging	0.62	1.00	0.98
Trend	0.67	0.98	1.00

CONCLUSION

This study comparison accuracy of different spatial interpolation methods based on GIS and Spearman correlation, the results show that the visualization effect of PM2.5 concentration spatial distribution by inverse distance weighted interpolation is best, while that of the trend surface is good, and ordinary kriging interpolation is general. The inverse distance weighted method is better than the other two methods whether it is from the error range of the forecast value, the accuracy of the predicting value relative to the observed value, or the sensitivity and the reflection of the simulated value. The correlation coefficient of simulated and observed value of is the largest by IDW is 0.99, in contrast, correlation coefficient of predicted and measured value are 0.62 and 0.67 by ordinary kriging and trend surface, indicating that correlation coefficient of trend surface and the ordinary kriging method has less precision than the inverse distance weighted method.

Acknowledgements

This research was supported by funding from the Scientific Research Program Funded by Shaanxi Provincial Education Department (Program No. 15JK1329), the PhD research start-up foundation of Xi`an Polytechnic University (No. BS1306), students' innovation and entrepreneurship training foundation at the provincial level of Xi`an Polytechnic University (No. 1234).

REFERENCES

[1] C. Hueglin, R. Gehrig, U. Baltensperger, M. Gysel, C. Monn and H. Vonmont. *Atmospheric Environment*, **2005**, 39(4), 637-651.

[2] A. van Donkelaar, R. V. Martin, R. J. Spurr and R. T. Burnett. *Environmental science & technology*, **2015**, 49(17), 10482-10491.

[3] X. Yao, C. K. Chan, M. Fang, S. Cadle, T. Chan, P. Mulawa, K. He and B. Ye. *Atmospheric Environment*, **2002**, 36(26), 4223-4234.

[4] C. Samara, D. Voutsa, A. Kouras, K. Eleftheriadis, T. Maggos, D. Saraga and M. Petrakakis. *Environmental Science and Pollution Research*, **2014**, 21(3), 1769-1785.

[5] P. Zhang, B. Hong, L. He, F. Cheng, P. Zhao, C. Wei and Y. Liu. *International journal of environmental research and public health*, **2015**, 12(10), 12171-12195.

[6] W. Shi, M. S. Wong, J. Wang and Y. Zhao. *Sensors*, **2012**, 12(6), 6825-6836.

[7] Y. Tang, T. Chai, L. Pan, P. Lee, D. Tong, H.-C. Kim and W. Chen. *Journal of the Air & Waste Management Association*, **2015**, 65(10), 1206-1216.

[8] B. Zou, M. Wang, N. Wan, J. G. Wilson, X. Fang and Y. Tang. *Environmental Science and Pollution Research*, **2015**, 1-10.

[9] L. Li, T. Losser, C. Yorke and R. Piltner. *International journal of environmental research and public health*, **2014**, 11(9), 9101-9141.

[10] C. A. Garcia, P.-S. Yap, H.-Y. Park and B. L. Weller. *International journal of environmental health research*, **2015**, 1-13.

[11] B. Zou, Y. Luo, N. Wan, Z. Zheng, T. Sternberg and Y. Liao. *Scientific reports*, **2015**, 5.

[12] L. Cordero, N. Malakar, Y. Wu, B. Gross and F. Moshary. *British Journal of Environment and Climate Change*, **2013**, 3(4), 547.

[13] M. Eeftens, R. Beelen, K. de Hoogh, T. Bellander, G. Cesaroni, M. Cirach, C. Declercq, A. Dedele, E. Dons and A. de Nazelle. *Environmental science & technology*, **2012**, 46(20), 11195-11205.

[14] B. S. Beckerman, M. Jerrett, M. Serre, R. V. Martin, S.-J. Lee, A. van Donkelaar, Z. Ross, J. Su and R. T. Burnett. *Environmental science & technology*, **2013**, 47(13), 7233-7241.

[15] K. F.-R. Liu, M.-J. Hung, J.-Y. Kuo and H.-H. Liang. *Journal of Geoscience and Environment Protection*, **2015**, 3(06), 20.